Antarct. Meteorite Res., **18**, 46–65, 2005

Rb-Sr and Sm-Nd dating of olivine-phyric shergottite Yamato 980459: Petrogenesis of depleted shergottites

Chi-Yu Shih[1*#], Laurence E. Nyquist[2], Henry Wiesmann[1†], Young Reese[3#] and Keiji Misawa[4]

[1]*Lockheed-Martin Space Operations, Mail Code C-23, 2400 NASA Parkway, P.O. Box 58561, Houston, TX 77258-8561, U.S.A.*
[2]*KR, NASA Johnson Space Center, 2101 NASA Parkway, Houston, TX 77058, U.S.A.*
[3]*Mail Code C-23, Hernandez Engineering Co., Houston, TX 77062, U.S.A.*
[4]*Antarctic Meteorite Research Center, National Institute of Polar Research, Kaga 1-chome, Itabashi-ku, Tokyo 173-8515*
[#]*current address: Jacobs/ESCG, Mail code JE-23, 2224 Bay Area Blvd., Houston, TX77058, U.S.A.*
[*]*Corresponding author. E-mail: chi-yu.shih1@jsc.nasa.gov*

(Received August 4, 2004; Accepted January 21, 2005)

Abstract: Martian meteorite Yamato (Y) 980459 has undergone terrestrial weathering in Antarctica. The weathering has affected the Sm-Nd isotopic system. Acid-washed pyroxenes, whole rock and quenched glass samples define a Sm-Nd isochron age of 472±47 (±2σ) Ma and a high initial ε_{Nd} value of +36.9±2.2 (±2σ). Both values are indisguishable from those reported for the other olivine-phyric depleted shergottite DaG 476. The Rb-Sr system of Y980459 shows even more terrestrial disturbance. The same acid-washed samples, which have a narrow Rb/Sr variation of only ~10%, do not yield an Rb-Sr isochron. However, the weighted average of nine samples yields a good initial $^{87}Sr/^{86}Sr$ ratio value of 0.701384±0.000021 (±2σ) at 472 Ma. This value is only slightly higher, by 1–2 ε-units, than that estimated from plagioclase data for DaG 476.

Calculations for a two-stage model for Sr and Nd isotopic evolution indicate that Y980459 came from a depleted mantle reservoir with $^{147}Sm/^{144}Nd$ = ~0.266 and $^{87}Rb/^{86}Sr$ = ~0.04, similar to the DaG 476 source. A three-stage model calculation suggests that the REE abundances and Nd isotopic systematics of Y980459 could be produced by partial melting of high $^{147}Sm/^{144}Nd$ garnet-rich residues which were formed after the extraction of LREE-rich, nakhlite-like melts from a postulated garnet-clinopyroxene-olivine source having $^{147}Sm/^{144}Nd$ = ~0.235.

key words: Yamato 980459, Rb-Sr, Sm-Nd, age, petrogenesis, nakhlite, depleted shergottite

1. Introduction

Martian meteorite Y980459 was found near the Minami-Yamato Nunataks, Antarctica by the Japanese Antarctic Research Expedition in 1998 and was recently classified as an olivine-bearing shergottite (Kojima and Imae, 2002; Misawa, 2003). It petrographically resembles many other olivine-phyric shergottites, *e.g.*, DaG 476/489,

[†] Deceased on January 9, 2004. His technical excellence will be missed by all coworkers.

SaU 005/094, Dhofar 019, NWA 1068/1110, NWA 1195, and EETA 79001 lith A (*e.g.*, Goodrich, 2002; Barrat *et al.*, 2002). This group of shergottites is characterized by variable crystallization ages from ~172 Ma to ~575 Ma and diverse ejection ages from ~1 Ma to ~20 Ma (*e.g.*, Nyquist *et al.*, 2001a,b). The majority of these olivine-phyric shergottites were found in hot Saharan and Arabian deserts where terrestrial weathering could have severely altered their chemical compositions and isotopic systematics. Y980459 is one of the few that were collected in Antarctica, a cold environment less prone to producing terrestrial weathering than hot deserts. Thus, key elemental and isotopic characteristics of the meteorite probably have been preserved since its fall to Earth. Y980459 is thus unique among these meteorites in several respects. It is apparently very fresh and only weakly shocked. Furthermore, it completely lacks plagioclase, but contains abundant residual volcanic glass, indicating that the meteorite crystallized very rapidly (*e.g.*, Greshake *et al.*, 2003; McKay and Mikouchi, 2003; McKay *et al.*, 2004). Thus, it may represent a volcanic melt that originated from the Martian mantle without undergoing much near-surface crystal fractionation.

QUE 94201, an olivine-free basaltic shergottite, as well as some olivine-phyric shergottites, *e.g.*, DaG 476, SaU 005 and Dho 019, have similar highly depleted-LREE patterns and distinctly high initial ε_{Nd} values and low initial $^{87}Sr/^{86}Sr$ ratios suggesting that they came from similar source regions highly depleted in LREE and Rb/Sr (Borg *et al.*, 1997, 2001; Nyquist *et al.*, 2001a,b). Thus, these basalts are herein referred to as *depleted shergottites*. In contrast, EETA lith A and NWA 1068 olivine-phyric shergottites have moderately to slightly depleted-LREE patterns, lower initial ε_{Nd} values, and higher initial $^{87}Sr/^{86}Sr$ ratios. These two basalts come from very different sources with lower Sm/Nd and higher Rb/Sr ratios, and are not members of the depleted shergottite group.

We performed Rb-Sr and Sm-Nd isotopic analyses on Y980459 to determine its crystallization age and the Sr and Nd isotopic signatures of its mantle source region. We have compared the results to those obtained for depleted shergottites and for the olivine-phyric shergottites EETA lith A and NWA 1068, respectively (Nyquist *et al.*, 2001a,b; Shih *et al.*, 2003b). Preliminary Rb-Sr and Sm-Nd isotopic data for Y980459 were presented at the International Symposium at NIPR, Japan, and at the 36th Lunar and Planetary Science Conference, USA (Shih *et al.*, 2003a, 2004). In this report, we present additional Rb-Sr and Sm-Nd isotopic data for Y980459 and discuss the petrogenesis of depleted shergottites.

2. Samples and analytical procedures

A sample of Y980459, weighing ~1.5 g, was kindly allocated by the National Institute of Polar Research of Japan for this study. The sample is a fine-grained rock containing yellow/brown olivine megacrysts. One fragment weighing ~0.5 g was used for this study and was processed by gently crushing and removing olivine megacrysts. Then the sample was further crushed to grain size $< 149\,\mu$m. About 100 mg of the sample was taken as a bulk rock sample (WR). The rest of the crushed sample was sieved into two size fractions, 149–74 μm and $< 74\,\mu$m, respectively. Mineral separations were made from the finer fraction sample (~95 mg) by density separation using the

heavy liquids bromoform, methylene iodide and Clerici's solutions. At $\rho > 3.45$ g/cm^3, we obtained a good yellow/brown olivine (Ol) sample of >95% purity. The white pyroxene-rich (Px1) and black glass-rich (Gl) samples were concentrated in the density fractions $\rho = 3.32$–3.45 g/cm^3 and $\rho = 2.85$–3.32 g/cm^3, respectively. A very small mesostasis-rich sample (~0.8 mg) was also obtained with $\rho < 2.85$ g/cm^3. Three more pyroxene-rich samples (Px2, 3, 4) were obtained from the 149–74 μm size fraction using both magnetic and density separation methods. Px2 was from the 0.4 ampere magnetic fraction of $\rho = 3.32$–3.45 g/cm^3. Px3 was from the 0.4 ampere non-magnetic fraction of $\rho = 3.32$–3.45 g/cm^3. Px4 was obtained from the 0.4 ampere magnetic fraction of $\rho = 2.85$–3.32 g/cm^3 by further fine crushing to <74 μm and density separation ($\rho < 3.32$ g/cm^3). In order to eliminate possible terrestrial contaminants, the samples of WR, Px, and Gl were washed with 2N HCl in an ultrasonic bath for 10 min. In addition, Px2 was further intensely washed with 3N HF following the procedure originated by Jagoutz (1989). The Ol and the $\rho < 2.85$ g/cm^3 samples were washed with less concentrated 0.5N HCl. Px2 (l) was a combined leachate sample collected from washes from three pyroxene samples (Px2, Px3 and Px4). Normally, 5–16% of the samples were leached out by the 2N HCl wash step. About 24% of the Px2 sample was lost to a stronger washing step using the combination of 2N HCl and 3N HF. However, the Ol and the $\rho < 2.85$ g/cm^3 samples lost the most amount of materials, ~30% and ~60%, respectively, even using a weak 0.5N HCl. Both the residues (r) and leaches (l) of these samples plus an unwashed WR sample were analyzed for Rb, Sr, Sm, and Nd. The detailed sample dissolution techniques and chemical procedures of Rb, Sr, Sm and Nd separations used in this study were reported previously (Nyquist *et al*., 1994; Shih *et al*., 1999). The total procedural blanks for Rb (~5 pg), Sr (~20 pg), Sm (~5 pg) and Nd (~10 pg) are low and negligible. All isotopic measurements were made on Finnigan-MAT mass spectrometers, either 261 or 262, following the procedures of Nyquist *et al*. (1994). The typical average value of $^{87}Sr/^{86}Sr$ for NBS 987 during the course of the study was 0.710231 ± 0.000027 ($2\sigma_p$, 9 analyses). The $^{87}Sr/^{86}Sr$ results reported here were renormalized to the NBS 987 $^{87}Sr/^{86}Sr = 0.710251$ of Nyquist *et al*. (1994). Sm and Nd isotopic compositions for all samples were measured as SmO^+ and NdO^+ ions, respectively, because of their low Sm and Nd abundances. The typical average value of $^{143}Nd/^{144}Nd$ for our Ames Nd standard, which has the same Nd isotopic ratio as the Caltech Nd standard *n* (Nd) β (Nyquist *et al*., 1994), during the course of the study was 0.511101 ± 0.000018 ($2\sigma_p$, 21 analyses of NdO^+ runs), normalized to $^{146}Nd/^{144}Nd = 0.724140$. The $^{143}Nd/^{144}Nd$ results for samples reported here were renormalized to $^{143}Nd/^{144}Nd = 0.511138$ for the Caltech Nd standard *n* (Nd) β given by Wasserburg *et al*. (1981).

3. Results and discussion

3.1. Sm-Nd isotopic results

The Sm and Nd analytical results for three whole rock and eleven mineral samples of shergottite Y980459 are given in Table 1. Figure 1 shows $^{147}Sm/^{144}Nd$ and $^{143}Nd/^{144}Nd$ data for three bulk rock and eight mineral samples, pyroxenes (Px), quenched glass (Gl) and olivines (Ol), for Y980459. One unwashed bulk rock (WR) and five

Table 1. Sm-Nd analytical results for olivine-phyric shergottite Y980459.

Sample[a]	wt (mg)	Sm (ppm)	Nd (ppm)	$^{147}Sm/^{144}Nd$[b]	$^{143}Nd/^{144}Nd$[b, c, e]
<100 mesh ($<149\,\mu$m)					
WR	27.15				
WR(r)	27.80		0.6		
WR(l)	3.05				
WR2	20.35	0.508	0.604	0.50812±56	0.514696±10
WR2(r)	19.35	0.600	0.713	0.50884±56	0.514713±18
WR2(l)	3.8	0.088	0.121	0.4398 ±58	0.51405 ±15
100–200 mesh (74–149 μm)					
Px2(r)	17.05	0.160	0.160	0.6052 ±14	0.514977±10
Px3(r)	8.4	0.079	0.085	0.5592 ±45	0.514851±14
Px4(r)	20.85	0.215	0.217	0.60014±96	0.514998±10
Px2(l)	8.78	0.317	0.420	0.45729±88	0.514452±10
<200 mesh ($<74\,\mu$m)					
<2.85(r)	0.35				
<2.85(l)	0.5				
Gl1(r)	25.5	0.856	1.026	0.50468±66	0.514673±15
Gl1(l)	3.0	0.090	0.134	0.4043 ±63	0.51375 ±15
Px1(r)	49.25	0.122	0.121	0.6086 ±10	0.514883±29
Px1(l)	2.4				
Ol1(r)	6.65	0.044	0.054	0.4901 ±84	0.514284±84
Ol1(l)	2.55				
Ames Nd standard:			NdO^+ (9 analyses 6/03):		0.511087±18[d]
			NdO^+ (6 analyses 8/03):		0.511096±12[d]
			NdO^+ (21 analyses 4–5/04):		0.511101±18[d]

[a] WR=whole rock, Px=pyroxene, Gl=Quenched glass, Ol=olivine, r=acid-washed residues, l=acid leachates.
[b] Uncertainties correspond to last figures and represent $\pm 2\sigma_m$ error limits.
[c] Normalized to $^{146}Nd/^{144}Nd=0.724140$ and adjusted to $^{143}Nd/^{144}Nd=0.511138$ of the Ames Nd standard (Wasserburg *et al*., 1981).
[d] Uncertainties correspond to last figures and represent $\pm 2\sigma_p$ error limits.
[e] Nd runs as NdO^+ mode.

acid-washed samples (WR(r), Gl(r) and Px2, 3, 4(r)) define a linear array corresponding to an age of 472±47 Ma for λ (^{147}Sm)=0.00654 Ga^{-1}, and an initial ε_{Nd} value=+36.9±2.2 using the Williamson (1968) regression program. The uncertainties for age and initial ε_{Nd} ratios are greater than those obtained previously for similar shergottites; *e.g*., DaG 476 (Borg *et al*., 2003) and QUE 94201 (Borg *et al*., 1997). This is primarily due to the fine-grained texture of Y980459. As noted in the petrographic studies, the shergottite contains 31% quenched glass materials produced during rapid cooling. Trace elements partitioning in coexisting mineral phases probably do not achieve complete equilibrium during such rapid crystallization. Thus, the total range in $^{147}Sm/^{144}Nd$ for data points along the isochron is only 20%, compared to ~100% for the DaG 476 isochron (see Fig. 2.). Also, the fine mineral grain sizes hinder clean mineral separation for analyses. It is unclear why the first washed pyroxene sample, Px1(r), deviates from this isochron by ~2 ε-units. Data for the subsequent replicate pyroxene samples, Px2(r) and Px4(r), including one severely washed with HF,

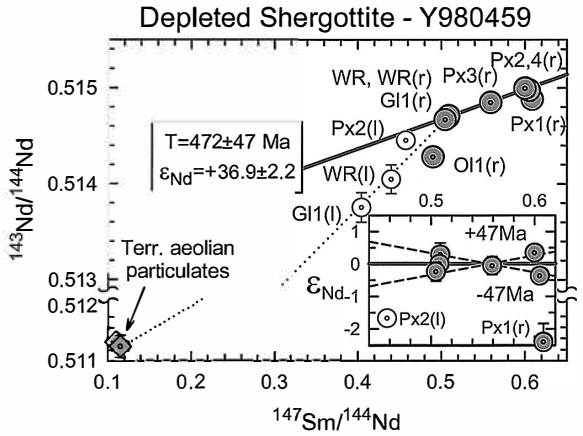

Fig. 1. Sm-Nd isotopic data for whole rock and mineral separates from Y980459 (circles). WR = whole rock, Gl = quenched glass, Px = pyroxene, Ol = olivine, r = residue after HCl wash and l = leachate after HCl wash (open circles). Six samples of whole rock, quenched glass and pyroxene separates define a linear array corresponding to an age of 472 ± 47 Ma for $\lambda(^{147}Sm) = 0.00654\,Ga^{-1}$ *and initial* $\varepsilon_{Nd} = 36.9 \pm 2.2$. *Leachates, Ol and Px1 are excluded from the regression. Three leachates plot below the isochron and are displaced towards the area defined by terrestrial river and aeolian particulates shown in diamonds (Goldstein et al., 1984; Albarede and Brouxel, 1987). Recent results of two Antarctic aerosols show* $^{143}Nd/^{144}Nd$ *ratios of ~0.51165 (Jagoutz et al., 2004). Those data can not be plotted on the figure because their respective Sm/Nd data are lacking. They can be good candidates of contaminants. The inserts show deviations of* $^{143}Nd/^{144}Nd$ *(in parts in* 10^{-4}*) for whole rock and mineral separates of Y980459 relative to the 473 Ma isochron. Dotted lines on either side of the best fit line correspond to* ±47 *Ma.*

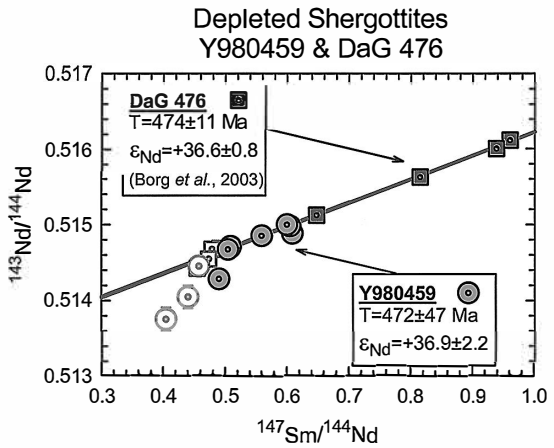

Fig. 2. Sm-Nd isotopic data for depleted shergottites Y980459 (circles, this study) and DaG 476 (squares, Borg et al., 2003). Solid symbols represent acid-washed samples and open symbols are acid washes. The isochrones defined for Y980459 and DaG 476 are coincident within error limits, suggesting these two shergottites were produced by a single igneous event on Mars.

Px2(r), are in good agreement with one another and differ from those of Px1(r). Accordingly, the Px1(r) sample was not included in the regression.

The age and initial ε_{Nd} value of Y980459 are in excellent agreement with those reported recently for desert shergottite DaG 476 (Borg *et al*., 2003; see Fig. 2) and unpublished JSC data for SaU 005. Y980459 is thus more closely related to DaG 476 and SaU 005 than to QUE 94201 and Dho 019. Data for Y980459 and DaG 476 define a single isochron for an age of 470±19 Ma and initial ε_{Nd} value = +37.0±1.0, suggesting these two shergottites were produced in a single igneous event on Mars. The short ^{10}Be cosmic-ray exposure age (1.1±0.2 Ma) also supports the close association of Y980459 to other olivine-phyric shergottites, DaG 476 and SaU 005 (Nishiizumi and Hillegonds, 2004). However, cosmic-ray exposure ages calculated from cosmogenic rare-gas ^{3}He, ^{21}Ne and ^{38}Ar yield an older average age of ~2.5 Ma for Y980459 resembling those of QUE 94201 and other enriched shergottites (Nagao and Okazaki, 2003; Christen *et al*., 2004).

Data for three leachates and the Ol samples plot significantly below the isochron and are displaced towards the data for terrestrial aeolian particulates (Goldstein *et al*., 1984; Albarede and Brouxel, 1987). These Sm-Nd isotopic data and high K and Br abundances in Y980459 reported recently (Dreibus *et al*., 2003) suggest that the meteorite may have been contaminated by terrestrial aerosols during residence in Antarctica. Comparison of the Y980459 data to those for DaG 476 suggests that the aberrant Px1(r) datum also was affected terrestrial contamination. Recent analyses of Antarctic aerosols extracted from snow yield ^{143}Nd/^{144}Nd ratios of ~0.51165 (Jagoutz *et al*., 2004), similar to those for non-Antarctic aerosols reported by Golsdstein *et al*. (1984). These aerosols also could be contaminants of Y980459.

3.2. Rb-Sr isotopic results

The Rb and Sr abundances and ^{87}Sr/^{86}Sr data for whole rocks and mineral separates are given in Table 2, and the ^{87}Rb/^{86}Sr and ^{87}Sr/^{86}Sr data for sixteen samples are shown in Fig. 3. These samples do not define a linear array, indicating an "open" Rb-Sr isotopic system. Nine samples of whole rock and mineral separates, including two unwashed whole rock samples (WR1, 2), two washed whole rock samples (WR1, 2(r)), four washed pyroxene samples (Px1, 2, 3, 4(r)), and one quenched glass sample (Gl(r)), have very similar ^{87}Rb/^{86}Sr and ^{87}Sr/^{86}Sr ratios despite their significant Rb and Sr concentration differences. The weighted average of these nine samples yields ^{87}Rb/^{86}Sr = 0.040±0.002 (±2σ) and ^{87}Sr/^{86}Sr = 0.701655±0.000029 (±2σ). The total lack of Rb/Sr fractionation among minerals and bulk rock samples of Y980459 makes the Rb-Sr mineral isochron study very difficult. However, assuming that the Sm-Nd age of 472 Ma represents the Y980459 age, we can calculate initial ^{87}Sr/^{86}Sr ratios for these nine samples at 472 Ma. The weighted average of model initial ^{87}Sr/^{86}Sr calculations yields 0.701384±0.000021 (±2σ). This value is a good estimate of initial ^{87}Sr/^{86}Sr for Y980459.

All five leachates and the acid-washed olivine sample plot far from the reference isochron and may have been disturbed by terrestrial contamination and/or weathering. The most likely contaminants of Antarctic meteorites are aerosols from snow. Recent Sr isotopic analyses of two Antarctic aerosols reveal high and variable ^{87}Sr/^{86}Sr ratios of

Table 2. Rb-Sr analytical results for olivine-phyric shergottite Y980459.

Sample[a]	wt (mg)	Rb (ppm)	Sr (ppm)	$^{87}Rb/^{86}Sr$[b]	$^{87}Sr/^{86}Sr$[b, c]
<100 mesh ($<149\,\mu$m)					
WR1	27.15	0.290	19.4	0.0432 ± 4	0.701703±43
WR(r)	27.80	0.262	20.3	0.0374 ± 3	0.701575±34
WR(l)	3.05	0.320	6.30	0.1468 ±14	0.704565±13
WR2	20.35	0.291	19.0	0.0443 ± 5	0.701698±10
WR2(r)	19.35	0.277	21.8	0.0368 ± 4	0.701598±14
WR2(l)	3.80	0.350	4.04	0.2509 ±32	0.704570±47
100–200 mesh (74–149 μm)					
Px2(r)	17.05	0.0500	3.78	0.03832±43	0.701639±10
Px3(r)	8.4	0.0346	2.33	0.04303±85	0.701704±13
Px4(r)	20.85	0.0775	5.53	0.04057±42	0.701640±10
Px2(l)	8.78	0.278	14.6	0.05501±57	0.702456±11
<200 mesh ($<74\,\mu$m)					
<2.85(r)	0.35	1.90	44.43	0.124 ± 2	0.701988±18
<2.85(l)	0.5				
Gl1(r)	25.5	0.426	32.99	0.0373 ± 4	0.701608±16
Gl1(l)	3.00	0.253	5.864	0.1248 ±15	0.705876±60
Px1(r)	49.25	0.0448	3.211	0.0404 ± 4	0.701715±23
Px1(l)	2.4	0.211	6.543	0.0933 ±13	0.7127 ± 6
Ol1(r)	6.65	0.0805	2.388	0.0975 ±14	0.70964 ±36
Ol1(l)	2.55				
NBS 987 Sr standard:			Sr^+ (9 analyses 4/03):		0.710224±26[d]
			Sr^+ (9 analyses 5/03):		0.710252±20[d]
			Sr^+ (6 analyses 7/03):		0.710262±32[d]
			Sr^+ (9 analyses 6/04):		0.710231±27[d]

[a] WR = whole rock, Px = pyroxene, Gl = Quenched glass, Ol = olivine, r = acid-washed residues, l = acid leachates.

[b] Uncertainties correspond to last figures and represent $\pm 2\sigma_m$ error limits.

[c] Normalized to $^{88}Sr/^{86}Sr = 8.37521$ and adjusted to $^{87}Sr/^{86}Sr = 0.710250$ of the NBS 987 Sr standard (Nyquist *et al*., 1994).

[d] Uncertainties correspond to last figures and represent $\pm 2\sigma_p$ error limits.

0.7101 and 0.7147 (Jagoutz *et al*., 2004). The high $^{87}Sr/^{86}Sr$ samples of Y980459 could be the results of contamination with these Antarctic aerosols.

The only sample plotting near the 472 Ma reference isochron is the washed low-density separate ($\rho < 2.85$(r)) sample. It plots slightly below the reference isochron by ~3 ε-units. The nine whole rock and mineral samples plus the $\rho < 2.85$(r) sample yield a tie-line age of 298±80 Ma for $\lambda(^{87}Rb) = 0.01402\,Ga^{-1}$ (Minster *et al*., 1982) and $^{87}Sr/^{86}Sr = 0.701484 \pm 0.000055$, resembling the age of the more evolved shergottite QUE 94201 (Borg *et al*., 1997). However, the validity of the tie-line age calculation depends heavily on the single analysis of the $\rho < 2.85$(r) sample, which was a rare small sample weighing only ~0.35 mg. Possibly the Rb-Sr systematics of this sample were also disturbed by contamination or during processing. Additional analyses of high Rb/Sr samples would be required to substantiate a Rb-Sr age younger than the Sm-Nd age.

If the Sm-Nd isochron age of 472 Ma represents the age of Y980459, the calculated

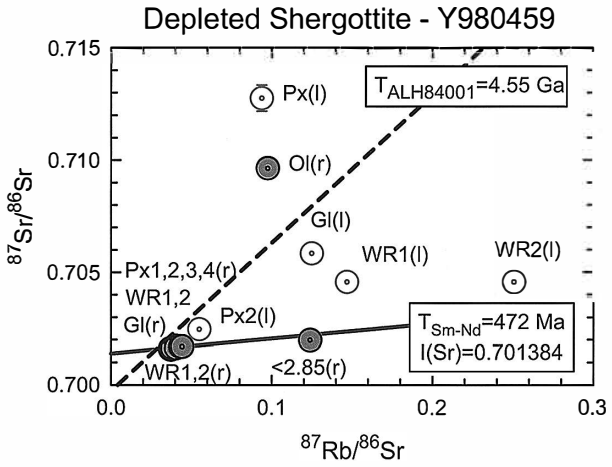

Fig. 3. Rb-Sr isotopic data for whole rock and mineral separates from Y980459 (circles). WR = whole rock, Gl = quenched glass, Px = pyroxene, Ol = olivine, <2.85 = separates of density $\rho < 2.85\,g/cm^3$, r = residue after HCl wash and l = leachate after HCl wash (open circles). No clear isochron can be derived from the data, suggesting severe alterations in the Rb-Sr system of the meteorite. A reference isochron $T_{Sm\text{-}Nd} = 472\,Ma$ (solid line) drawn for $\lambda(^{87}Rb) = 0.01402\,Ga^{-1}$ (Minster et al., 1982) and based on the Sm-Nd isochron age and the average value of the Rb-Sr isotopic data for nine WR, pyroxenes and quenched glass samples, yields a good estimate of initial $^{87}Sr/^{86}Sr = 0.701384 \pm 0.000021$ for Y980459. A 4.55 Ga reference isochron (dotted line) based on the Rb-Sr whole rock isochron of ALH 84001 (Nyquist et al., 1995) is also shown. Recent analyses of two Antarctic aerosols show variable $^{87}Sr/^{86}Sr$ values of 0.71013 and 0.71471 (Jagoutz et al., 2004). Those data can not be plotted on the figure because their respective Rb/Sr analyses are lacking. These aerosols are likely contaminants of Y980459.

initial $^{87}Sr/^{86}Sr$ value for Y980459 (0.701384) is slightly higher than for DaG 476 (0.701244) and SaU 005 (unpublished JSC data, 0.701294) by ~2 and ~1 ε-units, respectively. Using the age and initial Sr isotopic composition data, a single-stage evolution model calculation indicates that the time-averaged $^{87}Rb/^{86}Sr$ ratios for sources of Y980459, DaG 476 and SaU 005 are 0.041, 0.038 and 0.039, respectively. Thus, Y980459, DaG 476 and SaU 005 represent different flows produced contemporaneously from sources with similar but slightly different $^{87}Rb/^{86}Sr$ ratios. These sources are comparable to the source for the younger depleted shergottite QUE 94201 for which a source region $^{87}Rb/^{86}Sr$ ratio of 0.038 is calculated. Although differing slightly from one another, it is nevertheless interesting to note that those source region ratios are comparable to, but show less variability than those for the dominant olivine and pigeonite basalts at the Aopllo 12 lunar site, for example (Nyquist *et al*., 2001b).

3.3. Rare-earth element characteristics of olivine-phyric shergottites

CI-normalized REE distribution patterns for six olivine-phyric shergottites are plotted in Fig. 4. They include NWA 1068 (Barrat *et al*. 2002), EETA 79001 lith A (Laul, 1986), Dho 019 (Taylor *et al*., 2002), SaU 005 (Dreibus *et al*., 2000), DaG

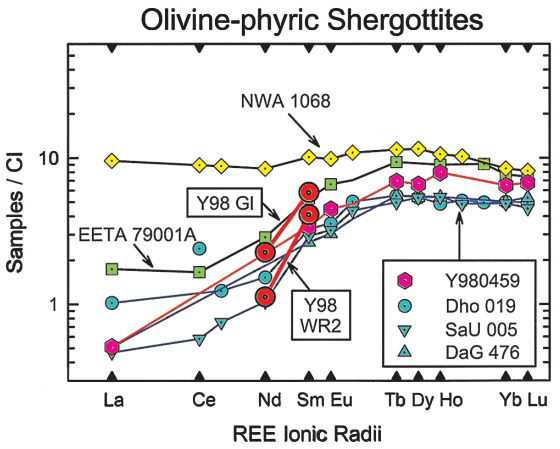

Fig. 4. CI-normailzed REE distributions for six olivine-phyric shergottites: NWA 1068 (diamonds; Barrat et al., 2002), EETA 79001 A (squares; Laul, 1986), Dho 019 (small circles; Taylor et al., 2002), SaU 005 (inverted triangles; Dreibus et al., 2000), DaG 476 (triangles; Zipfel et al., 2000) and Y980459 (large hexagons; Dreibus et al., 2003). Large circles are Sm and Nd data of whole rock (Y98 WR2) and quench glass (Y98 GI) for Y980459 from this work. The Sm concentration in Y98 WR2 is in adequate agreement with the Sm datum of Dreibus et al. (2003) for this meteorite, and slightly higher than Sm for SaU 005 and DaG 476. Dreibus et al. (2003) did not report Nd datum for Y980459, but our Nd datum combined with their La datum show that the relative LREE abundances in Y980459 must closely resemble those in SaU 005 and DaG 476. NWA 1068 has the least fractionated REE pattern. Y980459, Dho 019, SaU 005 and DaG 476 are all highly depleted in LREE, whereas EETA 79001 lith A is more moderately depleted in LREE. The unusually high Ce value in Dho 019, compared to its adjacent REEs, La and Nd, is likely the result of desert weathering (Dreibus et al., 2001).

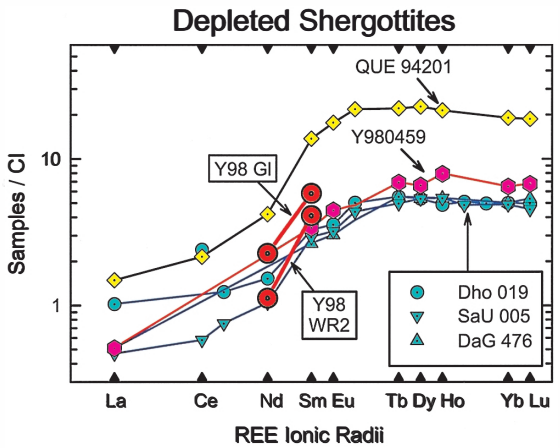

Fig. 5. CI-normalized REE distributions for five depleted shergottites: QUE 94201 (diamonds, Dreibus et al., 1996), Dho 019 (small circles), SaU 005 (inverted triangles), DaG 476 (triangles) and Y980459 (large hexagons). Data references are listed in Fig. 4 captions. All depleted shergottites have similar REE patterns highly depleted in LREE.

476 (Zipfel *et al*., 2000) and Y980459 (Dreibus *et al*., 2003). Also included are our Sm and Nd data of Y980459 whole rock and quenched glass. It is clear that not all olivine-phyric shergottites have similar REE patterns. The most noteworthy feature is that NWA 1068 exhibits a nearly unfractionated REE pattern and has the highest REE abundances. The other five olivine-phyric shergottites have similarly highly LREE-depleted patterns and lower REE abundances. The degree of LREE depletion for these samples diminishes as their REE absolute contents increase. The La (LREE) amounts among all the samples including NWA 1068 vary by almost 20-fold, whereas their HREE vary by only a factor of 2. The LREE variations among the basalts could be attributed to different degrees of partial melting from a common source. However, both crystallization and ejection age differences in Martian meteorites summarized in Nyquist *et al*. (2001a,b) suggest that these olivine-phyric shergottites are probably not all related to a single event. The REE pattern for Y980459 is very similar to those of Dho 019, SaU 005 and DaG 476. Age variations from ~474 to ~575 Ma for these four olivine-phyric rocks do not preclude their derivation from similar source regions, but clearly not from the same igneous event. Y980459 quenched glass contains about 50% more Sm and Nd than the whole rock and may represent a residual liquid produced during crystallization of the rock. The glass also has a slightly higher Sr/Nd value than the whole rock. Because Sr is usually concentrated in plagioclase, this suggests that the residual quenched glass would crystallize plagioclase if it cooled slowly. Thus, our trace element data are consistent with petrographic studies of the quench glass (*e.g*., McKay *et al*., 2004).

Figure 5 shows REE patterns for QUE 94201 and the four related olivine-phyric shergottites Y980459, DaG 476, SaU 005, and Dho 019. All these shergottites have distinctly LREE-depleted REE patterns. They could have derived from similar sources despite their age variations. Their respective sources are just as, or even more, depleted in LREE than the shergottites themselves because mineral/melt partitioning favors Sm over Nd for typical mantle source minerals, *e.g*., pyroxenes, garnets and perhaps olivines. Hence, these shergottites can be called *depleted shergottites*, meaning they came from sources highly depleted in LREE. Additional Sr and Nd isotopic evidence presented previously (*e.g*., Nyquist *et al*., 2001a,b) and later in the discussion clearly support the depleted nature of their source regions. Furthermore, the REE patterns of these shergottites resemble those of garnets (*e.g*., Green *et al*., 2000), strongly suggesting they were partial melts of garnet-bearing sources.

The overall REE abundance in QUE 94201 is higher than that in the other depleted shergottites by ~5-fold (Dreibus *et al*., 1996). QUE 94201 does not contain any olivine and has a very low mg-value (atomic Mg/(Mg+Fe)) of only 0.38 relative to 0.60–0.68 for the olivine-bearing members of this group. It may be derived from a parent melt similar to those of the other olivine-phyric depleted shergottites by olivine fractionation (*e.g*., Kring, 2002). It also may have been produced by a smaller degree of partial melting from a slightly different source, in agreement with its different crystallization age and Sr and Nd isotopic ratios.

3.4. Isotopic constraints on the sources of nakhlites and depleted shergottites

Sr and Nd isotopic characteristics for shergottite source regions can be illustrated

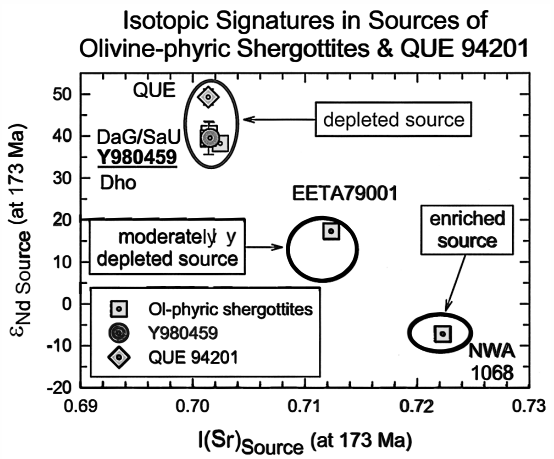

Fig. 6. Calculated $^{87}Sr/^{86}Sr$ vs. ε_{Nd} for Martian mantle source regions of the olivine-phyric shergottites (squares, and circle for Y980459) and QUE 94201 (diamond) at 173 Ma ago. Circled areas are source regions defined in Nyquist et al. (2001a,b) for the basaltic shergottites studied so far. Y980459, DaG 476, SaU 005, Dho 019 and QUE 94201 came from highly depleted sources. NWA 1068 and EETA 79001 are from enriched and moderately depleted sources, respectively. Thus, not all olivine-phyric shergottites came from a single source.

by their initial $^{87}Sr/^{86}Sr$ ratios and corresponding ε_{Nd} values at a common averaged age of 173 Ma for young shergottites (Nyquist *et al.*, 2001a,b), as shown in Fig. 6. Nyquist *et al.* (2001a,b) suggested that shergottites came from three major isotopically distinctive sources, i.e., enriched sources of $^{87}Sr/^{86}Sr = \sim 0.722$ and $\varepsilon_{Nd} = \sim -8$ (*e.g.*, Shergotty-type), moderately depleted sources of $^{87}Sr/^{86}Sr = \sim 0.712$ and $\varepsilon_{Nd} = \sim +10$ (*e.g.*, EETA-type) and highly depleted sources of $^{87}Sr/^{86}Sr = \sim 0.702$ and $\varepsilon_{Nd} = \sim +40$ (*e.g.*, QUE 94201-type). Using a two-stage evolution model, we can calculate $^{87}Rb/^{86}Sr$ ratios and corresponding $^{147}Sm/^{144}Nd$ ratios for these three types of sources. Their $^{87}Rb/^{86}Sr$ ratios for enriched, moderately depleted and highly depleted sources are ~0.36, ~0.21 and ~0.05, respectively. Their respective $^{147}Sm/^{144}Nd$ ratios are ~0.18, ~0.21 and ~0.27. As clearly shown in Fig. 6, not all olivine-phyric shergottites came from the same source. NWA 1068 came from an enriched source (Shih *et al.*, 2003b). EETA 79001 lith. A came from a source moderately depleted in LREE. The other four olivine-phyric shergottites (Y980459, DaG 476, SaU 005 and Dho 019) along with the evolved shergottite QUE94201 all came from more highly depleted sources. We reserve the term *depleted shergottites* for these five shergottites because of their distinctive severely depleted LREE patterns.

The $^{87}Rb/^{86}Sr$ for source regions of these depleted shergottites and for nakhlites can be estimated with the aid of the T(age)-initial $^{87}Sr/^{86}Sr$ diagram (Fig. 7), in which present-day and initial $^{87}Sr/^{86}Sr$ values are plotted for these meteorites at their respective crystallization ages. The calculated $^{87}Sr/^{86}Sr$ evolution prior to the crystallization ages of the meteorites is model dependent. We use a two-stage evolution model, the simplest model, which involves (1) the early differentiation of the Martian mantle during which

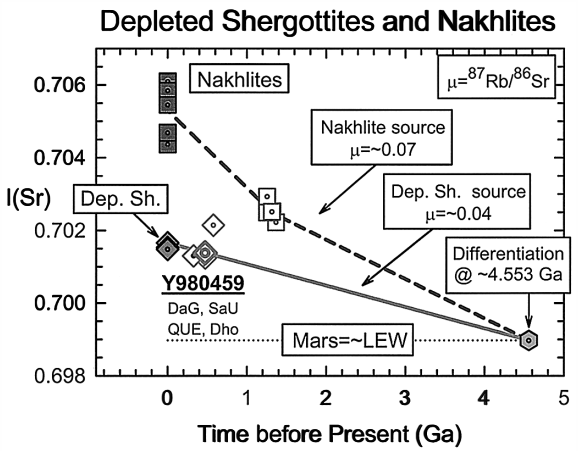

Fig. 7. T(age)-initial $^{87}Sr/^{86}Sr$ for depleted shergottites (diamonds) and nakhlites (squares). Nakhlite data are from Nakamura et al. (1982), Shih et al. (1998, 1999) and Misawa et al. (2003, 2005). The initial $^{87}Sr/^{86}Sr$ of Mars is assumed to be like that of the angrite LEW 86010 (0.698972 reported by Nyquist et al. (1994)). The lines represent time-integrated growth of $^{87}Sr/^{86}Sr$ from 4.553 Ga to formation times of 327–575 Ma for depleted shergottites (solid lines) and of 1.24–1.36 Ma for nakhlites (dashed lines). The slopes of the growth lines correspond to $^{87}Rb/^{86}Sr$ values in the mantle source regions and rocks themselves. A two-stage evolution model yields $^{87}Rb/^{86}Sr$ ~0.04 and ~0.07 for the source regions of depleted shergottites and nakhlites, respectively.

various source regions are produced, and (2) basalt formation at later times determined by the crystallization ages of the basalts. We further assume that the Martian mantle formed at T_0~4.553 Ga, which is ~13 Ma after solar system formation ~4.566 Ga ago based on the Martian core formation age using recent Hf-W studies by Yin *et al*. (2002). Also, we assume a mantle with a uniform Martian initial $^{87}Sr/^{86}Sr = 0.698972$, the value for angrite LEW86010 from Nyquist *et al*. (1994). This model yields source $^{87}Rb/^{86}Sr$ ratios of ~0.07 and ~0.04 for nakhlites and depleted shergottites, respectively. The $^{87}Sr/^{86}Sr$ ratios projected from the nahklite sources are ~0.7033 at the times of depleted shergottite formation ~300–600 Ma ago. This is too radiogenic to be characteristic of the sources of the depleted shergottites, which have $^{87}Sr/^{86}Sr$ ratios of ~0.7013 at those times. Thus, depleted shergottites can not be derived from the nakhlite sources.

The Rb/Sr fractionation at nakhlite formation ~1.3 ago is ~2.0 indicating that nakhlites can be formed by relatively small degrees of partial melting. In contrast, almost no Rb/Sr fractionation occurred at the times of depleted shergottite formation. Such small Rb/Sr fractionations can be achieved by large degrees of partial melting leaving residual phases that exclude Rb and Sr equally, such as olivines and orthopyroxenes.

Similarly, the $^{147}Sm/^{144}Nd$ for source regions of depleted shergottites and nakhlites can be calculated with the aid of the T(age)-initial ε_{Nd} diagram (Fig. 8). As in the Rb-Sr evolution, we have to assume the Martian mantle formed at T_0 = ~4.553 Ga with a uniform chondritic initial $^{143}Nd/^{144}Nd = 0.505893$ (CHUR, Jacobsen and Wasserburg,

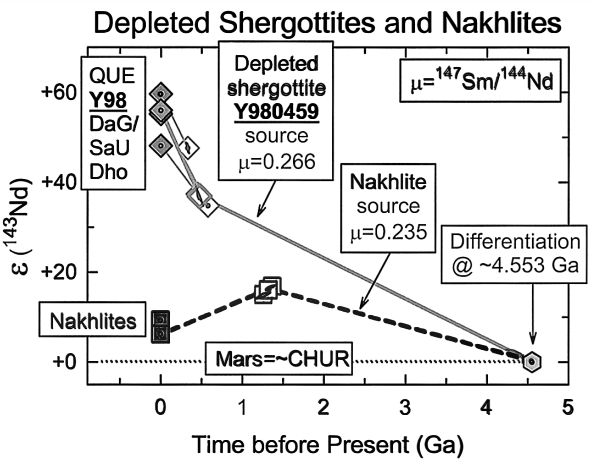

Fig. 8. T(age)-initial ε_{Nd} for depleted shergottites (diamonds) and nakhlites (squares). Lines represent the time-integrated growth in $^{143}Nd/^{144}Nd$, expressed in ε_{Nd} values, as derived from an initial Martian reservoir of chondritic $^{147}Sm/^{144}Nd$ and $^{143}Nd/^{144}Nd$ (CHUR) at 4.553 Ga (diamond) to the formation times of 327–575 Ma for depleted shergottites (solid lines) and of 1.26–1.37 Ma for nakhlites (dashed lines). The slopes of the lines correspond to $^{147}Sm/^{144}Nd$ ratios in the rocks and their respective mantle sources. A two-stage evolution model yields the $^{147}Sm/^{144}Nd$ source ratio of ~0.266 and ~0.235 for depleted shergottites and nakhlites, respectively.

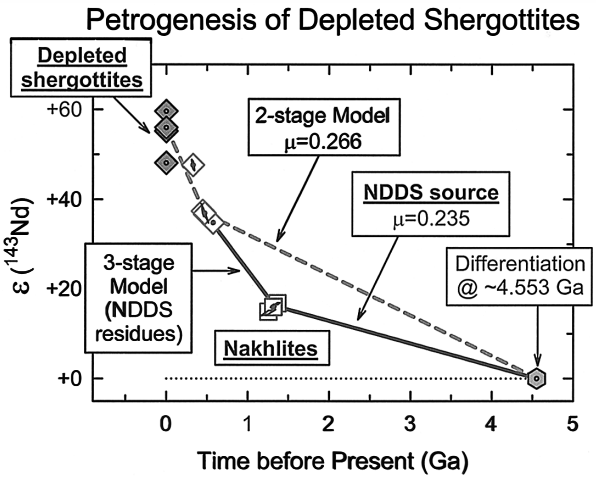

Fig. 9. T(age)-initial ε_{Nd} evolution during petrogenesis of depleted shergottites. A two-stage evolution model, shown in dashed lines, refers to (1) early formation of depleted shergottite sources at ~4.553 Ga and (2) the formation of depleted shergottites at 327–575 Ma (diamonds). Alternatively, a three-stage evolution model, shown in solid lines, refers to (1) early formation of Nakhlite Derived Depleted Shergottite (NDDS) sources at ~4.553 Ga, (2) the formation of nakhlite-like melts (open squares) accompanied by the formation of depleted shergottite sources (i.e., NDDS source residues) at 1.33 Ga, and (3) the final formation of depleted shergottites at 327–575 Ma.

1984). A two-stage model shows that the $^{147}Sm/^{144}Nd$ ratios for the sources of depleted shergottites and nakhlites are ~0.266 and ~0.235, respectively. Thus, both sources were depleted in LREE, and probably were comprised of mafic cumulates from the early Martian differentiation. The Sm/Nd fractionation at nakhlite formation, $(Sm/Nd)_{basalt}/(Sm/Nd)_{source}$ is ~0.60. This level of LREE enrichment in basalts indicates that the nakhlites can be melts formed by small degrees of partial melting. In contrast, severe Sm/Nd fractionations of a factor of ~2.0 are required at the formation of depleted shergottites. Such amounts of LREE *depletion* in basalts can only be achieved by crystal accumulation or by multiple episodes of remelting of residues near the formation times of depleted shergottites, as proposed for the formation of QUE 94201 by Borg *et al*. (1997).

Using a three-stage model allows us to propose an alternative way to achieve such magnitudes of Sm/Nd fractionation. The model, illustrated in Fig. 9, involves (1) early formation of Nakhlite-like Derived Depleted Shergottite, or NDDS, sources at ~4.553 Ga, (2) formation of depleted shergottite sources as residues after partial melting at ~1.3 Ga of sources similar to those of the nakhlites except for differing Rb/Sr ratios, and (3) formation of depleted shergottites with little fractionation of either Rb/Sr or Sm/Nd by large degrees of partial melting at ~300–600 Ma.

3.5. Petrogenesis of depleted shergottites

It has been argued that Mars experienced rapid accretion and early differentiation, accompanied by core-formation as indicated by enrichments of $\varepsilon^{142}Nd$ (Harper *et al*., 1995; Borg *et al*., 2003; Jagoutz *et al*., 2003) and $\varepsilon^{182}W$ (Lee and Halliday, 1997; Yin *et al*., 2002; Kleine *et al*., 2002) from decay of 103 Ma ^{146}Sm and 9 Ma ^{182}Hf, respectively, in Martian meteorites. This result can be interpreted if the Martian mantle is composed of stratified garnet-bearing cumulates produced by differentiation of the Martian magma ocean (Bertka and Fei, 1997; Agee and Draper, 2003), and probably followed by cumulate overturn (Hess, 2003; Elkins-Tanton *et al*., 2003). We assume here that NDDS sources are garnet-bearing cumulates (~garnet peridotites) composed of approximately 5–10% garnet, 5–10% clinopyroxene, and 80–90% olivine. These sources are depleted in LREE and assumed to have $^{147}Sm/^{144}Nd$ ratios of ~0.235 similar to those proposed previously for nakhlites (Nakamura *et al*., 1982; Shih *et al*., 1998, 1999). Results for the partial melting of such garnet-bearing NDDS sources are illustrated in the conventional T(age)-ε_{Nd} plot shown in Fig. 10. In this scenario, clinopyroxenes were consumed first in partial melting of garnet peridotites at high pressure following Yoder (1976). Therefore, these clinopyroxene-rich partial melts were similar to the parental nakhlite magmas, from which nakhlites crystallized by clinopyroxene accumulation (*e.g*., Nakamura *et al*., 1982). The $^{147}Sm/^{144}Nd$ ratios for these nakhlite-like parental magmas are estimated to be low at ~0.10–0.14 assuming 4–10% partial melting, thus matching well with those of nakhlites. In this calculation, we use the Sm and Nd partition coefficients (~0.15 and ~0.04, respectively) between garnet and melt reported by Draper *et al*. (2002). After the extraction of clinopyroxene-rich melts, the respective NDDS source residues are rich in garnet and have very high $^{147}Sm/^{144}Nd$ of 0.38–0.51. These garnet-rich NDDS source residues then could be sources capable of generating melts with garnet-like REE patterns by large degrees of partial melting

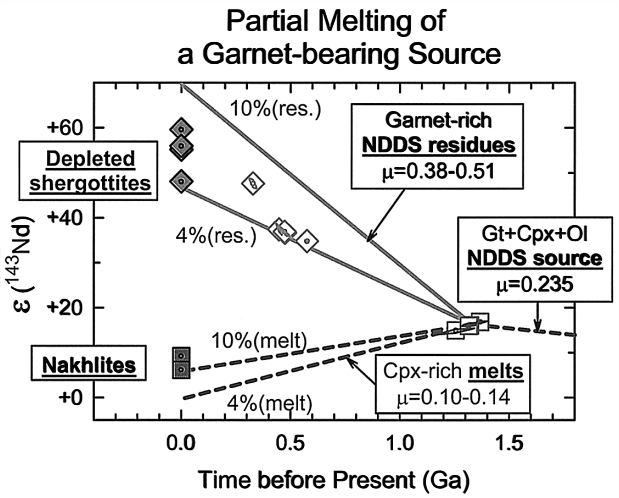

Fig. 10. Three-stage model for T(age)-initial ε_{Nd} evolution during petrogenesis of depleted shergottites. The model involves firstly the early formation of NDDS sources consisting of garnet-clinopyroxene-olivine with Nd = ~2 × CI and $^{147}Sm/^{144}Nd$ of ~0.235 at ~4.553 Ga. Secondly, the NDDS sources melted at ~1.26–1.37 Ga ago, forming clinopyroxene-rich melts of $^{147}Sm/^{144}Nd$ = 0.10–0.14 (similar to nakhlites) by 5–10% melting (dashed lines) and their corresponding garnet-rich NDDS residues having $^{147}Sm/^{144}Nd$ = 0.38–0.51, i.e., depleted shergottite sources shown in solid lines. Finally, melting of these garnet-rich residue sources at ~327–575 Ma formed the depleted shergottites themselves and left olivine-rich residues. In this model, little melt/source $^{147}Sm/^{144}Nd$ fractionation occurred during actual formation of depleted shergottites.

leaving most olivines as residues at later times ~300–600 Ma ago. When these melts crystallized, they would preserve the garnet-like REE pattern of depleted shergottites.

Results of the same partial melting calculations are illustrated in the REE distribution pattern diagrams shown in Figs. 11 and 12. For illustrations, we further assume that the NDDS sources have Nd concentrations of 2 × CI. Small degrees of partial melting (~9%) would produce LREE-enriched (low Sm/Nd) parent magmas of ~16 × CI. The nakhlites may have been clinopyroxene cumulates from similar melts, assuming that nakhlites crystallized with ~50% cumulus clinopyroxene and ~50% trapped melts. The calculated Sm and Nd concentration for such clinopyroxene cumulates match very well with those for nakhlites (Fig. 11). Additional extensive melting (~50 %) of garnet-rich NDDS source residues having Nd = ~0.6 × CI, leaving most olivine in the mantle, could have produced magmas with garnet-like REE patterns similar to those of the depleted shergottites (see Fig. 12). Similar ^{142}Nd excesses for depleted shergottites and nakhlites (*e.g.* Harper *et al.*, 1995; Jagoutz *et al.*, 2003) support this three-stage model and also suggest that Nd isotopic compositions in the NDDS source residues remained undisturbed or "closed" during the period between 1.3 Ga and ~300–600 Ma ago.

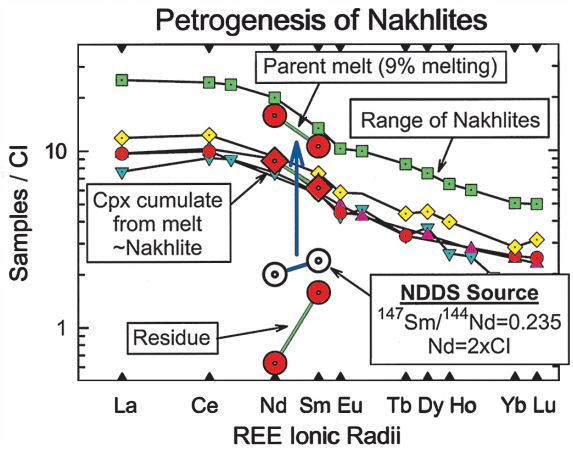

Fig. 11. CI-normalized REE distributions for the petrogenesis of nakhlites. Lines with small symbols are REE distribution patterns for five nakhlites (see Meyer (2003) for references). Sm and Nd are used for demonstration of REE partitioning during nakhlite genesis. Large open circles represent NDDS sources composed of garnet-clinopyroxene-olivine with Nd = 2 × CI and $^{147}Sm/^{144}Nd$ = ~0.235. Small-degree (~9%) melting of these sources produced clinopyroxene-rich parent melts with Nd = 16 × CI and $^{147}Sm/^{144}Nd$ = ~0.13. Calculated abundance patterns for rocks finally formed by 50% clinopyroxene accumulation match well with the observed REE distributions for nakhlites. The garnet-rich residues of Nd = ~0.6 × CI and $^{147}Sm/^{144}Nd$ = ~0.49 would be suitable sources of the depleted shergottites.

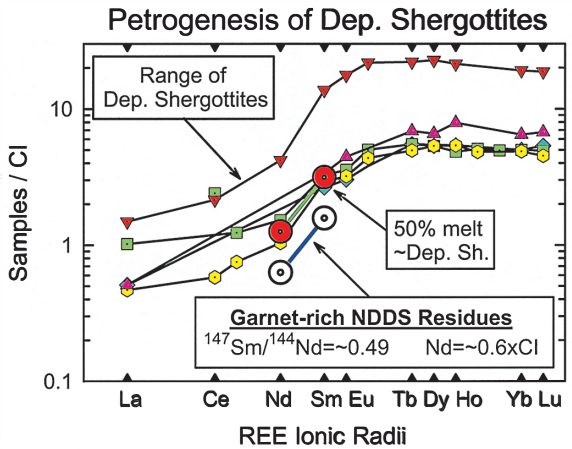

Fig. 12. CI-normalized REE distributions for the petrogenesis of depleted shergottites. Lines with small symbols are REE distribution patterns for five depleted shergottites (see Meyer (2003) for references). Sm and Nd are used for demonstration of the depleted shergottite genesis. Large open circles represent depleted shergottite sources (i.e., residues after extraction of melts resembling nakhlite parental melts or NDDS source) composed of garnet-olivine with Nd = ~0.6 × CI and $^{147}Sm/^{144}Nd$ = ~0.49. Large-degree melting (~50%) of these sources produced melts with Nd = 1.2 × CI and $^{147}Sm/^{144}Nd$ = ~0.49, matching well with the observed REE distributions for the depleted shergottites.

4. Conclusions

The Rb-Sr and Sm-Nd isotopic studies of olivine-phyric shergottite Y980459 lead to the following conclusions:

1) Although Y980459 was found in Antarctica, its Rb-Sr and Sm-Nd isotopic systems were nevertheless significantly altered by terrestrial contaminants. Thus, although terrestrial contamination is a more serious problem for hot desert meteorites, it also must be considered for Antarctic meteorites as well.

2) Acid-washed samples of whole rock, quenched glass and pyroxene define a Sm-Nd isochron age of 472 ± 47 Ma and initial ε_{Nd} value of $+36.9 \pm 2.2$, identical to values reported for DaG 476 (Borg *et al*., 2003).

3) Due to the rapid cooling of Y980459, no feldspar ever crystallized. Thus, samples of whole rock, quenched glass and pyroxene provide only a limited range in Rb/Sr ratios, which in turn do not yield an Rb-Sr isochron. Nevertheless, we have calculated the initial $^{87}Sr/^{86}Sr$ ratio of Y980459 based on the weighted average of nine whole rock and mineral samples to be 0.701384 ± 0.000021 at 472 Ma. QUE 94201, the only other depleted shergottite with a better-defined Rb-Sr isochron yields a similar initial $^{87}Sr/^{86}Sr$ of 0.701298 ± 0.000014 at 327 Ma (Borg *et al*., 1997).

4) The age and Sr and Nd isotopic data suggest that Y980459 is closely related to olivine-phyric shergottites DaG 476, SaU 005 and Dhofar 019 and to evolved olivine-free shergottite QUE 94201. All these rocks came from highly depleted sources in the Martian mantle. These isotopic data indicate that Y980459 is not related to olivine-phyric shergottites EETA lith A and NWA 1068, however.

5) A two-stage evolution model suggests Y980459 came from a depleted source region of time-averaged $^{147}Sm/^{144}Nd = 0.266$ and $^{87}Rb/^{86}Sr = 0.04$, which is more depleted than nakhlite sources. The calculated basalt/source fractionations of $^{147}Sm/^{144}Nd$ and $^{87}Rb/^{86}Sr$ at 472 Ma are 1.9 and 1.0, respectively. Such a high degree of $^{147}Sm/^{144}Nd$ fractionation can be achieved by multiple episodes of remelting of residues during basalt formation, as suggested previously by Borg *et al*. (1997) for the genesis of QUE 94201.

6) Alternatively, a three-stage model for the petrogenesis of Y980459 and other related depleted shergottites shows that they could be large-degree partial melts of garnet-rich residues of high $^{147}Sm/^{144}Nd = 0.4$–0.5. These garnet-bearing Nakhlite-like Derived Depleted Shergottite (NDDS) source residues, established ~1.3 Ga ago, were produced after the extraction of LREE-rich, nakhlite-like melts from depleted garnet-pyroxene-olivine sources with $^{147}Sm/^{144}Nd = 0.235$.

Acknowledgments

We are very grateful to the National Institute Polar Research (NIPR), Tokyo for providing the sample. Financial aid to C.-Y. Shih and L.E. Nyquist for attending *International Symposium—Evolution of Solar System Materials: A New Perspective from Antarctic Meteorites* at NIPR is very much appreciated. We are indebted to Profs. N. Nakamura and T. Swindle for thoroughly reviewing the manuscript. Finally, we thank the NASA Cosmochemistry Program and NIPR for funding the research.

Rerferences

Agee, C.B. and Draper, D.S. (2003): Melting of model martian mantle at high-pressure: Implications for the composition of the martian basalt source region. Lunar and Planetary Science XXXIV. Houston, Lunar Planet. Inst., Abstract #1408 (CD-ROM).

Albarede, F. and Brouxel, M. (1987): The Sm/Nd secular evolution of the continental crust and the depleted mantle. Earth Planet. Sci. Lett., **82**, 25–35.

Barrat, J.A., Jambon, A., Bohn, M., Gillet, P., Sautter, V., Goepel, C., Lesourd, M. and Keller, F. (2002): Petrology and chemistry of the picritic shergottite Northwest Africa 1068 (NWA 1068). Geochim. Cosmochim. Acta, **66**, 3505–3518.

Bertka, C.M. and Fei, Y. (1997): Mineralogy of the martian interior up to core-mantle boundary pressures. J. Geophys. Res., **102**, 5251–5264.

Borg, L.E., Nyquist, L.E., Taylor, L.A., Wiesmann, H. and Shih, C.-Y (1997): Constraints on martian differentiation processes from Rb-Sr and Sm-Nd isotopic analyses of the basaltic shergottite QUE 94201. Geochim. Cosmochim. Acta, **61**, 4915–4931.

Borg, L.E., Nyquist, L.E., Reese, Y., Wiesmann, H., Shih, C.-Y., Ivanova, M., Nazarov, M.V. and Taylor, L. A. (2001): The age of Dhofar 019 and its relationship to the other Martian meteorites. Lunar and Planetary Science XXXII. Houston, Lunar Planet. Inst., Abstract #1144 (CD-ROM).

Borg, L.E., Nyquist, L.E., Wiesmann, H., Shih, C.-Y. and Reese, Y. (2003): The age of Dar al Gani 476 and the differentiation history of the martian meteorites inferred from their radiogenic isotopic systematics. Geochim. Cosmochim. Acta, **67**, 3519–3536.

Christen, F., Busemann, H., Lorenzetti, S. and Eugster, O. (2004): Mars-ejection ages of Y-000593, Y-000749, and Y-000802 (paired nakhlites) and Y-980459 shergottite. Antarctic Meteorites XXVIII. Tokyo, Natl Inst. Polar Res., 6–7.

Draper, D.S., Xirouchakis, D. and Agee, C.B. (2002): Effect of majorite transformation on garnet-melt trace element partitioning. Lunar and Planetary Science XXXIII. Houston, Lunar Planet. Inst., Abstract #1306 (CD-ROM).

Dreibus, G., Spettel, B., Wlotzka, F., Schultz, L., Weber, H.W., Jochum, K.P. and Wanke, H. (1996): QUE 94201: An unusual Martian basalt. Meteorit. Planet. Sci., **31**, A39–A40.

Dreibus, G., Spettel, B., Haubold, R., Jochum, K.P., Palme, H., Wolf, D. and Zipfel, J. (2000): Chemistry of a new shergottite: Sayh al Uhaymir 005. Meteorit. Planet. Sci., **35**, A49.

Dreibus, G., Huisl, W., Haubold, R. and Jagoutz, E. (2001): Influence of terrestrial desert weathering in martian meteorites. Meteorit. Planet. Sci., **36**, A50–A51.

Dreibus, G., Haubold, R., Huisl, W. and Spettel, B. (2003): Comparison of the chemistry of Yamato 980459 with DaG 476 and SaU 005. International Symposium—Evolution of Solar System Materials: A New Perspective from Antarctic Meteorites. Tokyo, Natl Inst. Polar Res., 19–20.

Elkins-Tanton, L.T., Parmentier, E.M. and Hess, P.C. (2003): Magma ocean fractional crystallization and cumulate overturn in terrestrial planets: Implications for Mars. Meteorit. Planet. Sci., **38**, 1753–1771.

Goodrich, C. (2002): Olivine-phyric martian basalts: A new type of shergottite. Meteorit. Planet. Sci., **37**, B31–B34.

Goldstein, S.L., O'Nion, R.K. and Hamilton, P.J. (1984): A Sm-Nd isotopic study of atmospheric dusts and particulates from major river systems. Earth Planet. Sci. Lett., **70**, 221–236.

Green, T.H., Blundy, J.D., Adam, J. and Yaxley, G.M. (2000): SIMS determination of trace element partition coefficients between garnet, clinopyroxene and hydrous basaltic liquids at 2–7.5 GPa and 1080–1200°C. Lithos, **53**, 165–187.

Greshake, A., Fritz, J. and Stoeffler, D. (2003): Petrography and shock metamorphism of the unique shergottite Yamato 980459. International Symposium—Evolution of Solar System Materials: A New Perspective from Antarctic Meteorites. Tokyo, Natl Inst. Polar Res., 29–30.

Harper, C., Jr., Nyquist, L.E., Bansal, B.M., Wiesmann, H. and Shih, C.-Y (1995): Rapid accretion and early differentiation of Mars indicated by $^{142}Nd/^{144}Nd$ in SNC meteorites. Science, **267**, 213–217.

Hess, P.C. (2003): Origin of the martian crust and mantle. Unmixing the SNCs: Chemical, isotopic, and petrologic components of the martian meteorites. Lunar Planet. Inst., Cont. #1134, 23–24.

Jacobsen, S.B. and Wasserburg, G.J. (1984): Sm-Nd isotopic evolution of chondrites and achondrites, II.

Earth Planet. Sci. Lett., **67**, 137–150.
Jagoutz, E. (1989): Sr and Nd isotopic systematics in ALHA 77005: Age of shock metamorphism in shergottites and magmatic differentiation on Mars. Geochim. Cosmochim. Acta, **53**, 2429–2441.
Jagoutz, E., Dreibus, G. and Jotter, R. (2003): On the search for a neodymium-142 anomaly in terrestrial and martian rocks. International Symposium—Evolution of Solar System Materials: A New Perspective from Antarctic Meteorites. Tokyo, Natl Inst. Polar Res., 47–48.
Jagoutz, E., Bory, A., Jotter, R. and Zartman, R. (2004): Pb, Nd and Sr isotopes in aerosols extracted from snow, Berkner Island, Antarctica. Lunar and Planetary Science XXXV. Houston, Lunar Planet. Inst., Abstract #1530 (CD-ROM).
Kleine, T., Münker, C., Mezger, K. and Palme, H. (2002): Rapid accretion and early core formation on asteroids and terrestrial planets from Hf-W chronometry. Nature, **418**, 952–955.
Kojima, H. and Imae, N. (2002): Meteorite Newslett., **11** (1), 49 p.
Kring, D.A. (2002): QUE 94201: Reconsidering its origins as a bulk melt from a volcanic region of Mars. Unmixing the SNCs: Chemical, isotopic, and petrologic components of the martian meteorites. Lunar Planet. Inst., Cont. #1134, 31–32.
Laul, J.C. (1986): The Shergotty consortium and SNC meteorites: An overview. Geochim. Cosmochim. Acta, **50**, 875–888.
Lee, D.C. and Halliday, A.N. (1997): Core formation on Mars and differentiated asteroids. Nature, **388**, 854–857.
McKay, G. and Mikouchi, T. (2003): Crystallization of Antarctic shergottite Yamato 980459. International Symposium—Evolution of Solar System Materials: A New Perspective from Antarctic Meteorites. Tokyo, Natl Inst. Polar Res., 76–77.
McKay, G., Le, L., Schwandt, C., Mikouchi, T., Koizumi, E. and Jones, J. (2004): Yamato 980459: The most primitive shergottite? Lunar and Planetary Science XXXV. Houston, Lunar Planet. Inst., Abstract #2154 (CD-ROM).
Meyer, C., Jr. (2003): Mars Meteorite Compendium, NASA JSC#27672 Revision B, Houston.
Minster, J.F., Birck, J-L. and Allegre, C.J. (1982): Absolute age of formation of chondrites studied by the $^{87}Rb/^{87}Sr$ method. Nature, **300**, 414–418.
Misawa, K. (2003): The Yamato 980459 shergottite consortium. International Symposium—Evolution of Solar System Materials: A New Perspective from Antarctic Meteorites. Tokyo, Natl Inst. Polar Res., 84–85.
Misawa, K., Shih, C.-Y., Wiesmann, H. and Nyquist, L.E. (2003): Crystallization and alteration ages of the Antarctic nakhlite Yamato 000593. Lunar and Planetary Science XXXIV. Houston, Lunar Planet. Inst., Abstract #1556 (CD-ROM).
Misawa, K., Shih, C.-Y., Wiesmann, H., Garrison, D.H., Nyquist, L.E. and Bogard, D.D. (2005): Rb-Sr, Sm-Nd and Ar-Ar isotopic systematics of Antarctic nakhlite Yamato 000593. Antarct. Meteorite Res., **18**, 133–151.
Nagao, K. and Okazaki, R. (2003): Noble gases of Y980459 shergottite. International Symposium—Evolution of Solar System Materials: A New Perspective from Antarctic Meteorites. Tokyo, Natl Inst. Polar Res., 94.
Nakamura, N., Unruh, D.M., Tatsumoto M. and Hutchinson, R. (1982): Origin and evolution of the Nakhla meteorite inferred from the Sm-Nd and U-Pb systematics and REE, Ba, Sr, Rb and K abundances. Geochim. Cosmochim. Acta, **46**, 1555–1573.
Nishiizumi, K. and Hillegonds, D.J. (2004): Exposure and terrestrial histories of new Yamato lunar and martian meteorites. Antarctic Meteorites XXVIII. Tokyo, Natl Inst. Polar Res., 60–61.
Nyquist, L.E., Bansal, B., Wiesmann, H. and Shih, C.-Y. (1994): Neodymium, strontium, and chromium isotopic studies of the LEW86010 and Angra dos Reis meteorites and the chronology of the angrite parent body. Meteorit. Planet. Sci., **29**, 872–885.
Nyquist, L.E., Bansal, B., Wiesmann, H. and Shih, C.-Y. (1995): "Martian" young and old: Zagami and ALH 84001. Lunar Planetary Science XXVI. Houston, Lunar Planet. Inst., 1065–1066.
Nyquist, L.E., Bogard, D.D., Shih, C.-Y., Greshake, A., Stoffler, D. and Eugster, O. (2001a): Chronology and Evolution of Mars. Space Sci. Rev., **96**, 105–164.
Nyquist, L.E., Bogard, D.D. and Shih, C.-Y. (2001b): Radiometric chronology of the Moon and Mars. The

Century of Space Science, Vol. II, ed. By J. Bleeker *et al*. Kluwer, Acad. Pub., 1325–1376.

Shih, C.-Y., Nyquist, L.E., Reese, Y. and Wiesmann, H. (1998): The chronology of the nakhlite, Lafayette: Rb-Sr and Sm-Nd isotopic ages. Lunar and Planetary Science XXIX. Houston, Lunar Planet. Inst., Abstract #1145 (CD-ROM).

Shih, C.-Y., Nyquist, L.E. and Wiesmann, H. (1999): Samarium-neodynium and rubidium-strontium systematics of nakhlite Governador Valadares. Meteorit. Planet. Sci., **34**, 647–655.

Shih, C.-Y., Nyquist, L.E. and Wiesmann, H. (2003a): Isotopic studies of Antarctic olivine-phyric shergottite Y980459. International Symposium—Evolution of Solar System Materials: A New Perspective from Antarctic Meteorites. Tokyo, Natl Inst. Polar Res., 125–126.

Shih, C.-Y., Nyquist, L.E., Wiesmann, H. and Misawa, K. (2003b): Age and petrogenesis of picritic shergottite NWA 1068. Lunar and Planetary Science XXXIV. Houston, Lunar Planet. Inst., Abstract #1439 (CD-ROM).

Shih, C.-Y., Nyquist, L.E., Wiesmann, H. and Misawa, K. (2004): Rb-Sr and Sm-Nd isotopic studies of shergottite Y980459 and a petrogenetic link between depleted shergottites and nakhlites. Lunar and Planetary Science XXXV. Houston, Lunar Planet. Inst., Abstract #1814 (CD-ROM).

Taylor, L.A., Nazarov, M.A., Shearer, C.K., McSween, H.Y., Jr., Cahill, J. *et al*. (2002): Martian meteorite Dhofar 019: a new shergottite. Meteorit. Planet. Sci., **37**, 1107–1128.

Wasserburg, G.J., Jacobsen, S.B., DePaolo, D.J., McCulloch, M.T. and Wen, T. (1981): Precise determination of Sm/Nd ratios, Sm and Nd isotopic abundances in standard solutions. Geochim. Cosmochim. Acta, **45**, 2311–2323.

Williamson, J.H. (1968): Least-squares fitting of a straight line. Can. J. Phys., **46**, 1845–1847.

Yin, Q., Jacobsen, S.B., Yamashita, K., Blichert-Toft, J., Telouk, P. and Albarede, F. (2002): A short timescale for terrestrial planet formation from Hf-W chronometry of meteorites. Nature, **418**, 949–952.

Yoder, H.S., Jr. (1976): Generation of Basaltic Magma. Washington, D.C., National Academy of Sciences, 265 p.

Zipfel, J., Scherer, P., Spettel, B., Dreibus, G. and Schultz, L. (2000): Petrology and chemistry of the new shergottite Dar al Gani 476. Meteorit. Planet. Sci., **35**, 95–106.